Bulgarian Geophysical Journal, 2001, Vol.27, No.1-4, pp.85-103

Ionospheric Electron Content model based on a steady-state theoretical profiler: I. Mathematical formulation

S. M. Stankov

Geophysical Institute, Bulgarian Academy of Sciences, Sofia 1113, Bulgaria

Abstract. The Total Electron Content (TEC), and the Ionospheric Electron Content (IEC) giving the ionosphere contribution to the TEC, are integral profile characteristics of utmost significance for various space-weather issues. The interest towards these characteristics was recently rejuvenated thanks to the development of the Global Positioning System (GPS) which, among other advantages, provides opportunity for a relatively cheap way of permanent monitoring the topside ionosphere and plasmasphere on a global scale. Several TEC models have been developed during the years, ranging from purely theoretical to completely empirical types. In the broad spectrum of the models, there is a pronounced need of a new semi-empirical model that can represent more realistically the topside electron profile – area traditionally preserved for simple ionospheric models like the Chapman layer. Presented is a new semi-empirical type Ionospheric Electron Content model (IECM) based on a steady-state theoretical 'ionospheric profiler' and tied to oxygen-hydrogen ion transition level measurements. The mathematical code of the profiler is composed of coupled continuity and momentum equations of the three basic ions in the upper ionosphere – the O^+, H^+, and He^+ ions, which densities are calculated along magnetic field lines. The obtained total ion density is used for computing the electron content. The development database is built on longterm observations using the U.S. Navy Navigation Satellite System (NNSS). The IECM can be effectively used for both single-site calculations and regional mapping. If ionosonde measurements are available on a real-time basis, the presented model can be upgraded with advanced operational-mode features.

Keywords: electron content, mathematical model, ion transition level

1. Introduction

The Total Electron Content (TEC), together with the F2 - layer maximal electron concentration (N_mF2), is one of the most important quantitative characteristics of the ionosphere and the altitude electron profile in particular. The TEC gives the total ionisation which can be used in various geophysical long-term and short-term studies including radio-wave propagation, geomagnetic / ionospheric storms, gravity waves, solar flare effects, etc. Global or regional models of the total electron content are very important for the trans-ionospheric radio system operation. There are three basic approaches to producing TEC maps:

a) *Empirical* modelling: using TEC values from either observations of radio beacon signals or derived from ion/electron density measurements;

b) *Theoretical* modelling: integrating the electron density obtained from 'first principle' (theoretical) models of the ionosphere-plasmasphere system;

c) *Semi-empirical* modelling: integrating an electron density profile to one (or more) profile characteristics, for example the density peak obtained from a numerical map of the critical frequency.

The purpose of this publication is to present a new semi-empirical TEC model based on a steady-state theoretical 'profiler' and oxygen-hydrogen ion transition level (O^+-H^+ TL) measurements. The mathematical code of the profiler is composed of coupled continuity and momentum equations of the most important ion constituents in the upper ionosphere – the O^+, H^+, and He^+ ions. These densities are calculated along magnetic field lines and consequently the vertical total ion (electron) density is derived. The aim is to produce a vertical electron density profile of high quality and then to integrate it numerically in order to derive the electron content up to a given ceiling height. Because the major contribution comes from the ionosphere, and because a large amount of data have been accumulated from NNSS the emphasis here is on the ionosphere contribution to TEC, i.e. the ionospheric electron content (IEC). The construction of the IEC model is built upon the theoretical profiler tied to the empirically obtained values of the upper transition level. A semi-empirical model like the one presented in this paper could significantly help the understanding of the complex structure and physical processes of the topside ionosphere and plasmasphere.

This paper is organised in the following way. First, some notes are provided on the electron content theory and methods of observation. Next, the general structure of the IEC model is described. Further, the mathematical formulation of the theoretical profiler is presented in detail. Finally, some exemplary IECM calculations are demonstrated.

2. Ionospheric Electron Content – theory and observations

The (columnar) electron content is the number of electrons in a column of one square metre cross section along the ray path from the transmitting satellite to the receiving station. Therefore, the *slant* electron content, I_s , is defined as the (line) integral of the electron density

$$I_s = \int_T^R N_e(s)ds$$

where $N_e(s)$ is the electron concentration at a given point on the raypath, ds is the differential element along the ray path TR from transmitter (T) to the receiver (R). The slant electron content must be converted to the equivalent vertical electron content, I_v , in order to compare contents from ray paths with different elevation angles. Hence, the vertical electron content is defined as the height integral of the electron density from the height of the receiving station up to the 'ceiling height' h_c (the height of the transmitting satellite or infinity):

$$I_v = \int_T^R N_e(h)dh$$

where dh is the height element. If the upper boundary is infinity than the vertical electron content is called 'total'. The term 'ionospheric electron content' is usually reserved for the electron content measurements using satellites flying below about 2000 km. The geometry of IEC measurement using NNSS is given in **Fig.1**.

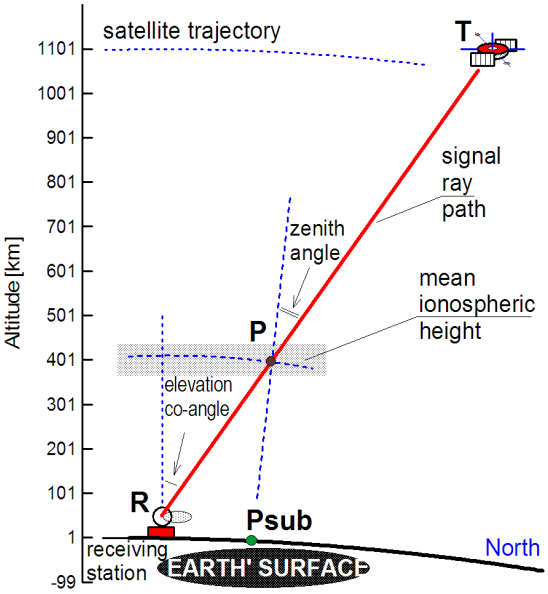

Fig.1 NNSS-based IEC measurements

The *vertical* electron content is more convenient especially when comparison with other types of data is required. It is also more important than the slant value, since equivalent vertical values are more easily related to other geophysical measurements such as to ground-based vertical incidence sounding (ionosonde) and incoherent scatter radar measurements. A standard method of converting from slant to vertical IEC is to multiply the

slant value by the cosine of the zenith angle at some mean ionospheric height h_{mean} (usually chosen at 50 km above hmF2) along the ray path and assign this vertical value to the 'sub-ionospheric' point P_{sub} . After replacing the path element ds with -dh/cosχ and extracting the mean value out of the integral, the slant to vertical conversion yields:

$$I_s = \int_T^R N_e(s)\,ds = \int_0^{h_s} N_e(h)\,\frac{1}{\cos\chi}\,dh = \overline{\frac{1}{\cos\chi}} \int_0^{h_s} N_e(h)\,dh = G_M \int_0^{h_s} N_e\,dh = G_M\, I_v$$

where χ is the zenith angle at the mean ionospheric point P (the point of the ray path at h_{mean}). The 'geometric factor' G_M (i.e. the value of 1/cosχ at the mean ionospheric height) is an approximation of the true mean value of 1/cosχ . In general, the conversion procedure is quite complicated due to the height and shape of the electron density profile and the existing horizontal gradients of TEC.

All modern electron content measurement techniques (Dieminger et al., 1995) rely on quantifying the propagation effects on the signal phase. With geometric optics, the received signal phase is theoretically expressed by the following formula:

$$\phi = \frac{2\pi\, f}{c} \int_T^R n\,ds + 2\pi\, f\, t$$

where f is the transmitted frequency, n is the refractive index, c – the light's velocity, t – time, and ds is the ray path element. The refractive index depends on the transmitted frequency; a convenient approximation (for $f > 40$ MHz) is

$$n^2 = 1 - f_p^2 \,/\, \left(f^2 \pm f\, f_g \left|\cos\Theta\right|\right) \quad , \quad f_p^2 = \frac{e^2}{4\pi m \varepsilon_0} N_e \quad , \quad f_g = \frac{e}{2\pi m} B$$

where f_p is plasma frequency, f_g - gyrofrequency of free electrons, Θ - the angle between the phase propagation vector and the vector of geomagnetic induction, e – electron charge [As], m –electron mass [kg], ε_0 –free-space permitivity [$Asm^{-1}V^{-1}$], B – geomagnetic induction [Vsm^{-2}], A=80.6[m^3s^{-2}]. Three are the major methods for TEC evaluation: Faraday, Differential-Doppler and Group-Delay methods.

The *Faraday effect* (the magneto-plasma effect on the polarization plane of a linearly polarized radio signal) is observed when the magnetic field and electron density along the ray path jointly cause the polarization rotation. A signal with an arbitrary polarization can be split into right-hand and left-hand circular components, yielding the following formula:

$$\Omega = \phi_L - \phi_R = \frac{2\pi\, f}{c} \int_T^R (n_R - n_L)\,ds = f^{-2} K_F \overline{M} \int_0^{hc} N_e\,dh$$

where $K_F \approx 47295.7$ [$m^2s^{-2}T^{-1}$] and $\overline{M}$ is the mean value of $B\left|\cos\Theta\right| / \cos\chi$ at the 'mean ionospheric height' of (usually) 400km. The Faraday effect observations

have been carried out with satellites on geo-stationary orbits (ATS-6, SIRIO), with zero inclination, periods of 24 hours, and altitude of approximately 36,000 km. The main advantage of this system is that it provides the total electron content including the plasmasphere contribution.

The *Differential Doppler effect* (Carrier phase difference) requires two carriers transmitted phase-coherently. If f_1 and f_2 are the frequencies ($f_1 = pf_r$, $f_2 = qf_r$, f_r – reference frequency, *p,q*-whole numbers), the phase difference ψ is estimated as follows

$$\psi = \phi_2 / q - \phi_1 / p \; = \frac{2\pi f_r}{c} \int_T^R (n_2 - n_1)\, ds = G_M \int_0^{hc} N_e\, dh$$

where G_M is the geometric factor. The most famous system used for Differential Doppler observations is the Navy Navigation Satellite System, consisting of nearly circular low-altitude (~1100km) polar orbiting (1.5 hours period) satellites. The main advantage of this system is that it provides the important latitude dependence of the ionospheric electron content for essentially the same time.

The *Group Delay effect* (Modulation phase difference) is the most recently developed technique and can be used in various modification. It is based on two carrier frequencies f_1 and f_2, which are amplitude-modulated by a sine wave with frequency f_m. Two sidebands ($f_1 \pm f_m$, $f_2 \pm f_m$) are produced for each carrier but only one is used at a time, and four signal components are separately received (f_1, $f_{\pm 1} = f_1 \pm f_m$, f_2, $f_{\pm 2} = f_2 \pm f_m$) with corresponding phases (ϕ_1, $\phi_{\pm 1}$, ϕ_2, $\phi_{\pm 2}$). The following phase combination (using the lower sideband), is proportional to the 'group delay':

$$\Phi = (\phi_1 - \phi_{-1}) - (\phi_2 - \phi_{-2}) \; = \frac{2\pi}{c} \int_T^R (f_1 n_1 - f_{-1} n_{-1} - f_2 n_2 + f_{-2} n_{-2})\, ds$$

For $f_2 >> f_1$ and $f_1 >> f_m$, the value of Φ is proportional to the slant electron content. The Global Positioning System (GPS) is a recently-developed system of satellites orbiting the Earth at a height of about 20000 km, with inclinations of 55° and time periods of 12 hours. GPS can be used for TEC measurements based on the Group Delay effect and with the help of the system's frequency channels of L_1 = 1575.42 MHz and L_2 = 1227.6 MHz. Basic advantages of the GPS-based measurements are: give the total electron content up to the plasmapause, provide global coverage, and use sufficiently high frequencies to ensure that the ionospheric absorption and geomagnetic field effects on the radio signals are small.

A major problem associated with all of the above types of measurements is that additional information is needed to deduce the electron content from the propagation effects. This is due to the ambiguity introduced by the fact that signal phases are measurable modulo 2π only. Also, the ionosphere is not adequately represented by the thin shell model used in the slant-to-vertical conversion.

3. Ionospheric Electron Content model – general structure

The presented Ionospheric Electron Content Model (IECM) is based on three separate modules - a steady-state theoretical model for the topside (above hmF2) electron profile, an analytical model for the bottom-side part of the electron profile, empirical model of the upper transition level, and input parameter model.

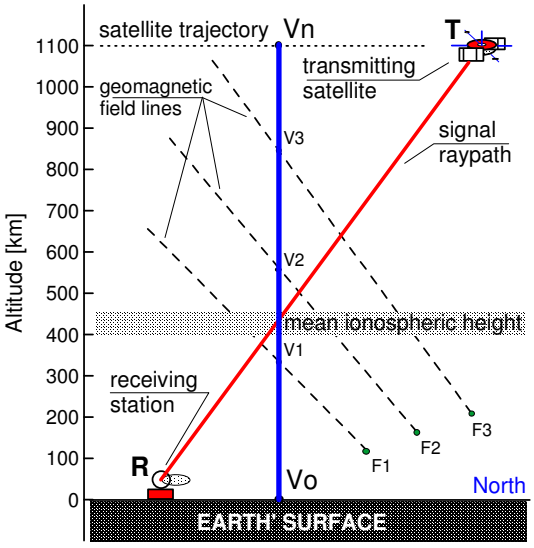

Fig.2 Geometry of the IEC model calculations

Auxiliary parts include the outside data sources, such as empirical models (MSIS, IRI), ionosonde and satellite in-situ measurements of densities and temperatures. Input parameters are all neutral atmosphere characteristics plus the initial values for the theoretical profiler. The aim of the IECM is to produce the vertical electron content at a given point and at a specified time (**Fig.2**). This task is carried out in two major stages – first, calculation of the electron density along the vertical above the chosen location, and second, numerical integration of these densities using quadrature formulae. It is important to mention that the steady-state theoretical model (used for the top-side profile) calculates the ion densities along a given dipole field line. In order to obtain the vertical density distribution along the chosen vertical V_0V_n, there are two options. One is to calculate the field line distribution and convert it to the vertical using a formula depending on the inclination; such conversion is not reliable at lower latitudes. The other option, chosen for this model, is in the following. According to the desired integration quality, a grid (V_1,V_2, ...) is set onto the vertical V_0V_n. There is only one field line passing through each of the grid points. Thus, a unique set of field lines is determined, along which the steady-state model should be run starting from the 'foot points' F_1, F_2, F_3, ... at 200 km altitude up to arbitrary heights above the altitude of V_n. During these computations a reference is made to the upper transition level which helps the model particularly at sunrise and sunset periods. After extracting the required electron densities at the grid points, the top-side vertical profile is obtained. Identifying hmF2 and NmF2, the bottom-side profile is calculated using the Epstein ionospheric layer.

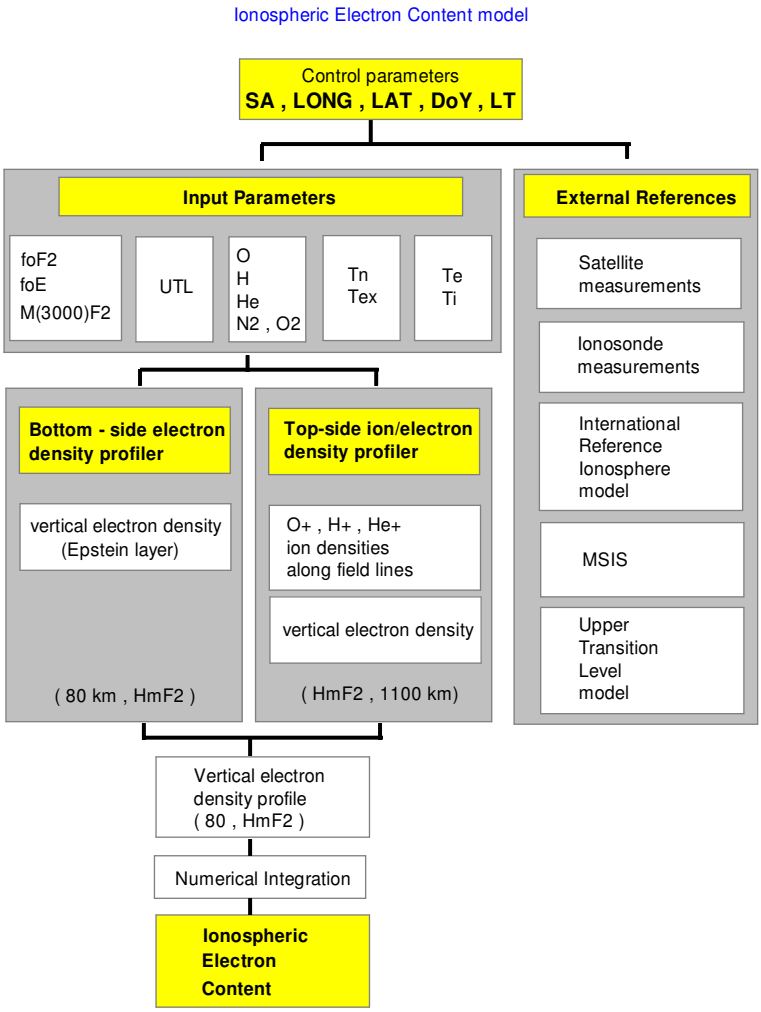

Fig.3 Ionospheric Electron Content model structure

Having obtained the vertical electron density distribution, the numerical integration of the profile is straightforward.

The presented model is designed primarily for the ionospheric electron content, i.e. up to 1100 km but can be extended to further altitudes if required. The general scheme of the model calculations has a modular structure (**Fig.3**) allowing high flexibility when using input parameters from various sources and much easier modifications and upgrading.

4. Bottom-side theoretical profiler

Previous IEC studies using theoretical modelling (Stankov, 1994) suggest that the bottom-side profile (below the F-layer peak electron density height, hmF2) should be more precisely modelled, and if possible connected to measurements of the ground vertical ionospheric soundings. In this part, a reliable and flexible way of profiling the bottom-side electron density distribution will be described.

The information about the bottom-side part of the profile and the electron peak density and peak height is taken from either ionosonde measurements if available, empirical maps, or from the already calculated topside profile (notice that topside profiles can be calculated starting from 150-250km up to an arbitrary height).

The vertical electron density distribution below hmF2 is calculated with the 'Epstein layer' model:

$$N_e(h) = N_e(h_m)\, sech^2\left(\frac{h - h_m}{B_{bot}}\right)$$

where $N_e(h)$ is the electron density, B_{bot} is the bottom-side thickness, and

$$sech(h) = 1/\cosh(h) \quad , \quad \cosh(h) = 0.5\left(\exp(h) + \exp(-h)\right).$$

Required ionosonde parameters are the F2–layer critical frequency (foF2), the propagation factor ($M_{3000}F2$), and the E–layer critical frequency (foE). The F2-layer peak height is estimated using the expression (Dudeney, 1983):

$$hmF2 = -176 + 1470\frac{M_{3000}F2\left\{(0.0196 M_{3000}F2^2 + 1)/(1.296 M_{3000}F2^2 - 1)\right\}^{1/2}}{M_{3000}F2 - 0.012 + 0.253/(foF2/foE - 1.215)}$$

The bottom-side thickness, B_{bot}, is calculated by (Di Giovanni and Radicella, 1990): $B_{bot} = 0.385.N_m F2.(dN/dh)^{-1}_{\max}$, where $(dN/dh)_{\max}$ is the value of the gradient of $N_e(h)$ at the base of the F2 layer, and it is determined by the following formula:

$$(dN/dh)_{\max} = \exp\left(-3.467 + 0.857 \ln(foF2)^2 + 2.02 \ln(M_{3000}F2)\right)$$

When F2 and E layers are both present in the ionograms, the bottom-side profile is constructed as a sum of two identical Epstein layers (Rawer, 1988):

$$N(h) = 4\, N_m \exp((h - h_m)/B_{bot})\, ((1 + \exp((h - h_m)/B_{bot})^{-2},$$

where N_m and h_m are the (F2- or E-) layer's peak density and peak height respectively. The electron density distribution at D region heights is not modelled in detail.

The F2-layer critical frequency, foF2, is easily deduced from the peak density, obtained from the top-side theoretical profile, using the standard conversion formula $NmF2[m^{-3}] = 1.24\times10^{10}\times(foF2[MHz])^2$.

The E-layer critical frequency, foE, can be calculated by the following formula (Dieminger et al., 1995): $foE(R,\phi,\chi) = (ABCD)^{1/4}$, where R is the sunspot number, ϕ is the geographic latitude, and χ is the solar zenith angle. The components A and B express the solar activity, C - latitudinal, and D - diurnal dependence:

$A = 0.0091R$

$B = (\cos \chi_{noon})^{m}$ $\quad m = 1.93 + 1.92 \cos\phi$, for $|\phi|<32°$; $\quad m = 0.11 - 0.49 \cos\phi$, for $|\phi|\geq 32°$

$C = X + Y \cos \phi$ $\quad X = 23$, $Y = 116$, for $|\phi|<32°$; $\quad X = 92$, $Y = 35$, for $|\phi|\geq 32°$

$D = (\cos \chi)^{p}$ $\quad p = 1.31$, for $|\phi|\leq 12°$; $\quad p = 1.20$, for $|\phi|>12°$

In the IEC model, the foE at night is set to zero.

The propagation factor M(3000)F2 is taken from ionosonde data, empirical maps, or deduced after fitting the Epstein layer to the (150, hmF2) part of the topside theoretical profile. Exemplary reconstruction of the bottom-side

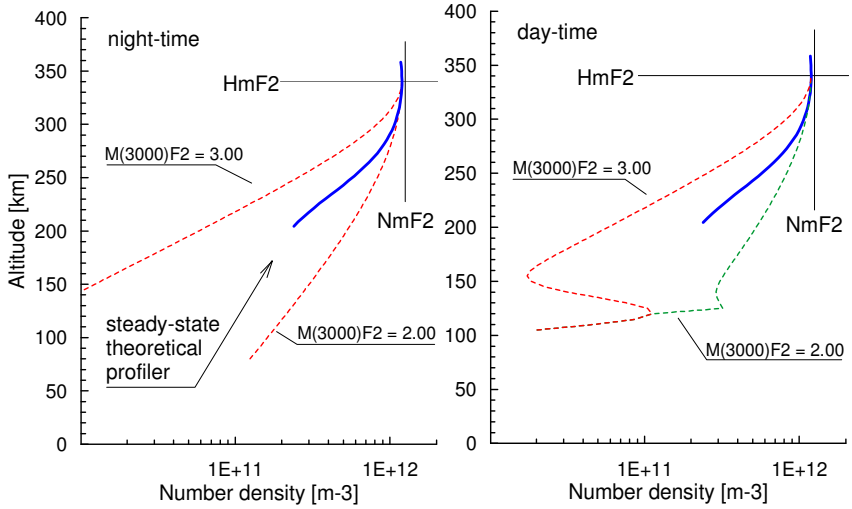

Fig.4 Bottom-side electron density profiles obtained by the Epstein layer (dashed line) and the steady-state profiler (solid line) for night-time (left) and day-time (right).

profile is given below in the **Fig.4** for night-time and day-time conditions.

Notice the effect of the M(3000)F2 on the electron profile. By varying the M(3000)F2 value, the Epstein layer can be fitted to the bottom part of the steady-state model profile.

5. Top-side theoretical profiler

The steady-state mathematical model of the upper ionosphere (Stankov, 1994; Stankov, 1996a) has been developed mainly for utilizing satellite measurements for purposes of ion composition studies, ionospheric mapping, ionospheric storm studies, etc. (Kutiev and Stankov, 1996; Stankov, 1996b).

The model geometry employs the concept of a plasma flux tube having the profile of centred–dipole magnetic field line passing the tube at a given moment. The Earth's magnetic induction field **B** is defined by

$$B = 0.311\frac{r_e^3}{r^3}\left(1+3\sin^2\theta\right)^{0.5}$$

and the field line is then $r = r_{eq}\cos^2\vartheta$, where r is the radial distance from the Earth's centre, r_e is the Earth's radius, r_{eq} is the equatorial radial distance of the magnetic field line, θ is the dipole latitude.

2.1 System of equations

The model is based on the equations of continuity, momentum and energy balance for the O^+ , H^+ and He^+ ions using a centred dipole approximation to the Earth's magnetic field. It calculates the individual ion concentrations and velocities, ion and electron temperatures along a specified field line from a start altitude (~150 km) up to an arbitrary altitude.

The ion continuity equation, parallel to the field line, is

$$B\frac{\partial}{\partial s}\left(\frac{1}{B}n_i v_i\right) = P_i - L_i$$

where n_i is the ion concentration, v_i – ion field-aligned velocity, P_i – ion production rate, L_i - ion loss rate, s – arc length along the field line.

The momentum equation is derived from the Boltzmann equation in magneto-hydrodynamic approximation and has the form:

$$m_i g\sin I + \frac{kT_i}{n_i}\frac{\partial n_i}{\partial s} + k\left(1-\alpha_i\right)\frac{\partial T_i}{\partial s} + \frac{kT_e}{n_e}\frac{\partial n_e}{\partial s} + k\frac{\partial T_e}{\partial s} +$$

$$+ m_i\nu_{in}\left(v_i - v_n\right) + m_i\nu_{in}\left(v_i - v_n\right) + \sum_{\substack{j=1\\ j\neq i}} m_i\nu_{ij}\left(v_i - v_j\right) = 0$$

where k is the Boltzmann's constant, n_i - ion concentration, n_e – electron concentration, m_i – ion mass, v_i – ion field aligned velocity, v_w – neutral wind field aligned velocity, ν_{ij} – collision frequency between i and j ion species, ν_{in} –

collision frequency between $i^{\text{-th}}$ ion and its neutral parent species , T_i – ion temperature, T_e – electron temperature.

The electron temperature is calculated by the following formula based on the heat conduction along the flux tube:

$$T_e(h) = T_e(h_b)\left\{1 + 3.5(h - h_b)\left[\frac{d}{dh}(\ln T_e)\right]_{h_b}\right\}^{2/7}$$

where h_b is the base height.

The ion temperature is calculated from the formula:

$$T_i(h) = \frac{T_n(h) + \eta(h)[T_e(h)]^{-0.5}}{1 + \eta(h)[T_e(h)]^{-1.5}} \quad , \quad \eta(h) = 0.1\times 10^{13}\left(\sum_{j=1}^{5}\eta_j(h)\right)^{-1}$$

where $\eta_j(h)$ are the concentrations of the neutral species O, H, He, N_2, O_2, and $\eta(h)$ is the total neutral concentration.

An alternative way of calculating the minor hydrogen and helium ions concentrations under chemical-equilibrium conditions is by using the following formulae (Banks and Kockarts, 1973):

$$n(H^+) = 1.125\frac{\eta(H)}{\eta(O)}\left(\frac{T_n}{T_i}\right)^{0.5} n(O^+)$$

$$n(He^+) = \frac{\mathrm{I(He)}\,\eta(He)}{c_1\eta(N_2) + c_2\eta(O_2)}$$

where the term I(He)η(He) represents the direct photoionization of the neutral helium and c1,c2 are rate coefficients.

Other convenient way of obtaining the H+ and He+ concentrations is through the empirically deduced formulae for the height distribution of the H^+/O^+ and He^+/O^+ density ratios R_i :

$$R_i(h,\lambda) = a_i h^{c_i\lambda + d_i}\exp(b_i\lambda) \quad , \quad i = 1(H^+/O^+),\ 2(He^+/O^+)$$

where h is the height, λ is the dipole latitude, and the coefficients a_i , b_i , c_i , d_i are determined from satellite in-situ measurements (Stankov, 1994; Kutiev and Stankov, 1994; Stankov, 1996b; Stankov, 1996c).

5.2 Input parameters

The model system is not self consistent and requires several quantities as input parameters - the neutral atmosphere, neutral wind, solar EUV flux, etc.

Assuming barometric law distribution, the concentration of a given neutral species is calculated from

$$\eta_j(h) = \eta_j(h)\frac{T_n(h_b)}{T_n(h)}\exp\left(-\frac{h-h_b}{H_j}\right)$$

where H_j is the scale height, T_n is the temperature of the neutral gas, h_b is the base height usually at 300 km.

Based on the exospheric temperature T_{ex} , the temperature of the neutral gas is determined from the following expressions:

$$T_n(h) = T_{ex} + (a_1 T_{ex} - a_2)(h - h_b) + a_3(h_p - h_a)^{0.5} \quad , \quad h \in (150, h_a)$$
$$T_n(h) = T_{ex} - a_3(h_p - h_a)^{0.5} + a_4(h - h_a)^{0.5} \quad , \quad h \in (h_a, h_p)$$
$$T_n(h) = T_{ex} \quad , \quad h \in (h_p, +\infty)$$

where h_a=200km, h_p=27+0.327T_{ex}, $a_1 = 8.75\times10^{-3}$, $a_2 = 1.75$, $a_3 = -9.428$, $a_4 = 9.48$.

5.3 Numerical solution

The model system of equations is solved numerically by using predictor-corrector methods, starting from a given height h_s (150-200km), where initial values are provided from outside the model, e.g. satellite measurements. The required initial value of $n_s(O^+)$ at the starting height can also be deduced from the chemical equilibrium condition P_i=L_i for day-time calculations. Alternatively, a searching procedure is developed for automatically finding the boundary values in a self-consistent manner. The technique is rather complicated (Stankov, 1996) and relies on strict control of the ion fluxes and the high sensitivity of the solution from the initial values.

The upper integration height is freely chosen, which is very convenient when calculating the total electron content.

It is important to mention that the points distribution along the vertical can be arbitrary; if necessary at low altitudes the grid points could be only 5-10 km apart, while the points at higher altitudes can be much further apart - up to 100 km without increasing the error (Stankov, 1990).

6. The oxygen-hydrogen (upper) ion transition level

The relative abundance of hydrogen ions is a significant factor affecting the topside electron density profile, hence the O^+-H^+ transition level can be successfully utilized as a reference point.

long	0 - 60	60 - 120	120 - 180	180 - 240	240 - 300	300 - 360	0 - 60	60 - 120	120 - 180	180 - 240	240 - 300	300 - 360
lat	***summer** : night-time*						***summer** : day-time*					
55-65	824	824	824	824	824	824	1248	1200	1152	1152	1200	1248
45-55	765	770	765	771	775	780	1237	1189	1142	1142	1189	1237
35-45	725	730	730	735	739	739	1198	1152	1106	1106	1152	1198
25-35	714	726	732	730	727	726	1128	1085	1042	1042	1085	1128
15-25	718	714	714	712	710	714	1035	995	955	955	995	1035
5 -15	749	745	745	745	745	745	988	950	893	893	950	988
0	765	765	765	765	765	765	978	940	903	903	940	978
-15 -5	750	750	750	750	754	750	986	948	911	911	948	986
-25-15	724	722	720	724	728	724	1012	973	935	935	973	1012
-35-25	715	713	710	709	702	709	1043	1002	962	962	1002	1043
-45-35	730	735	739	739	725	730	1104	1061	1019	1019	1061	1104
-55-45	775	781	785	790	775	780	1136	1092	1049	1049	1092	1136
-65-55	824	824	824	824	824	824	1144	1100	1056	1056	1100	1144
lat	***winter** : night-time*						***winter** : day-time*					
55-65	754	754	754	754	754	754	1078	1078	1100	1122	1122	1100
45-55	740	735	741	741	751	745	1070	1070	1092	1113	1113	1092
35-45	705	720	724	720	705	705	1040	1040	1061	1082	1082	1061
25-35	645	650	653	646	645	645	982	982	1002	1022	1022	1002
15-25	625	627	628	632	625	625	954	954	973	992	992	973
5 -15	715	715	715	713	711	709	929	929	948	967	967	948
0	766	762	762	762	762	762	918	918	936	955	955	936
-15 -5	750	748	754	754	754	752	930	930	949	968	968	949
-25-15	690	690	690	692	693	697	959	959	978	998	998	978
-35-25	635	635	635	640	643	636	994	994	1014	1034	1034	1014
-45-35	670	670	670	685	689	685	1049	1049	1070	1091	1091	1070
-55-45	725	719	716	709	715	715	1073	1073	1095	1117	1117	1095
-65-55	754	754	754	754	754	754	1078	1078	1100	1122	1122	1100

Table 1. The O^+- H^+ transition height model's data base for *low solar activity* (R=50): night-time (left side) and day-time (right side) values [km] for summer (top) and winter (bottom) seasons.

Here, the transition level is determined from a model (Kutiev *et al*., 1994), based on satellite in-situ measurements of the individual O^+ and H^+ ion densities. The model was recently upgraded (using averaged profiles from AE-C data) to provide longitudinal variations during LSA day-time conditions. The data is approximated by a multi-variable polynomial for conveniently referencing the level with respect to the basic spatial and temporal parameters.

long	0 - 60	60 - 120	120 - 180	180 - 240	240 - 300	300 - 360	0 - 60	60 - 120	120 - 180	180 - 240	240 - 300	300 - 360
lat	***summer** : night-time*						***summer** : day-time*					
55-65	1100	1100	1100	1100	1100	1100	1430	1430	1430	1430	1430	1430
45-55	922	912	902	922	942	932	1420	1420	1420	1420	1420	1420
35-45	950	940	930	940	950	950	1380	1380	1380	1380	1380	1380
25-35	1011	991	981	976	971	991	1300	1300	1300	1300	1300	1300
15-25	1040	1030	1030	1025	1020	1030	1250	1250	1250	1250	1250	1250
5-15	1049	1039	1039	1039	1039	1039	1200	1200	1200	1200	1200	1200
0	1050	1040	1040	1040	1040	1040	1150	1150	1150	1150	1150	1150
-15 -5	1080	1090	1090	1090	1090	1090	1200	1200	1200	1200	1200	1200
-25-15	1050	1050	1050	1070	1070	1070	1250	1250	1250	1250	1250	1250
-35-25	1000	1000	1000	1020	1030	1030	1330	1330	1330	1330	1330	1330
-45-35	970	970	970	1030	1040	1040	1380	1380	1380	1380	1380	1380
-55-45	1060	1060	1060	1070	1080	1080	1420	1420	1420	1420	1420	1420
-65-55	1100	1100	1100	1100	1100	1100	1430	1430	1430	1430	1430	1430
lat	***winter** : night-time*						***winter** : day-time*					
55-65	910	910	910	910	910	910	1363	1363	1363	1363	1363	1363
45-55	880	900	900	908	916	917	1293	1293	1293	1293	1293	1293
35-45	721	729	731	736	736	738	1224	1224	1224	1224	1224	1224
25-35	672	679	682	685	685	689	1200	1200	1200	1200	1200	1200
15-25	667	660	660	653	653	660	1190	1190	1190	1190	1190	1190
5-15	687	680	680	680	680	680	1170	1170	1170	1170	1170	1170
0	1000	1000	1000	1000	1000	1000	1150	1150	1150	1150	1150	1150
-15 -5	1028	978	948	948	948	948	1170	1170	1170	1170	1170	1170
-25-15	686	686	686	726	766	726	1180	1180	1180	1180	1180	1180
-35-25	660	660	660	695	730	690	1200	1200	1200	1200	1200	1200
-45-35	731	731	731	811	881	811	1220	1220	1220	1220	1220	1220
-55-45	998	898	848	938	998	998	1293	1293	1293	1293	1293	1293
-65-55	1100	1100	1100	1100	1100	1100	1363	1363	1363	1363	1363	1363

Table 2. The O^+-H^+ transition height model data base for *medium solar activity* (R=100): night-time (left side) and day-time (right side) values for summer (top) and winter (bottom) seasons.

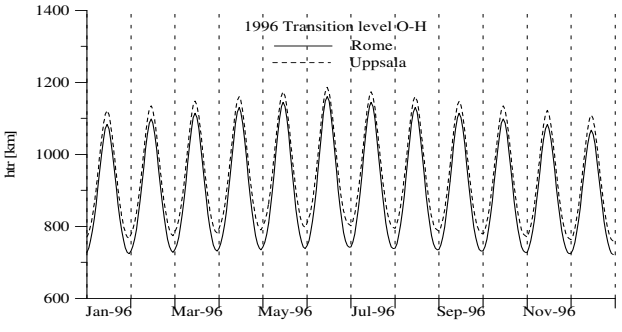

Fig.5 The modelled O^+-H^+ TL annual behaviour.

The method of least-squares fit is applied for determining the polynomial coefficients. Some example results are given in **Fig.5** for low solar activity conditions and for sites at different latitudes - Rome (12.5E,41.8N) and Uppsala (17.6E,59.8N).

7. Results and discussion

Exemplary results from the IEC model calculations are presented in this part for equinox and middle solar activity (F10.7=140) at middle geomagnetic latitudes (40°N). The model was run along several dipole lines which 'foot points'

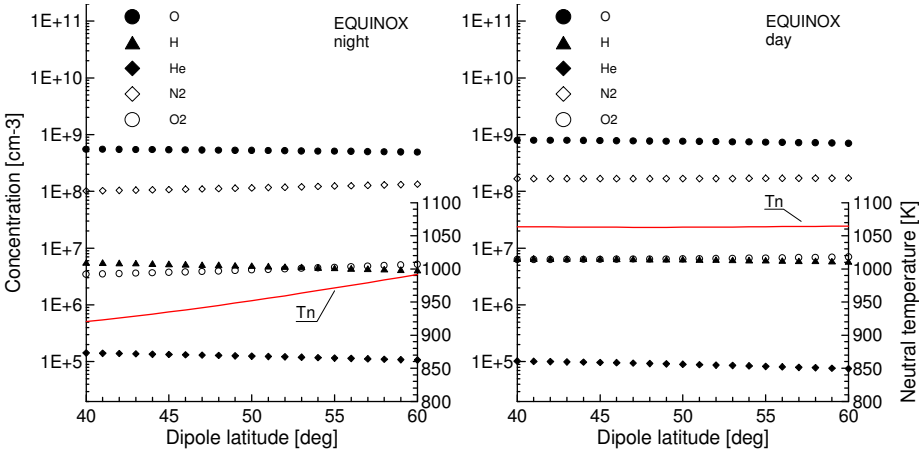

Fig.6 The MSIS neutral atmosphere parameters for September equinox at middle solar activity (F10.7=140) for night-time (left) and day-time (right) conditions.

at 300 km altitude are within the range 40-60°N.

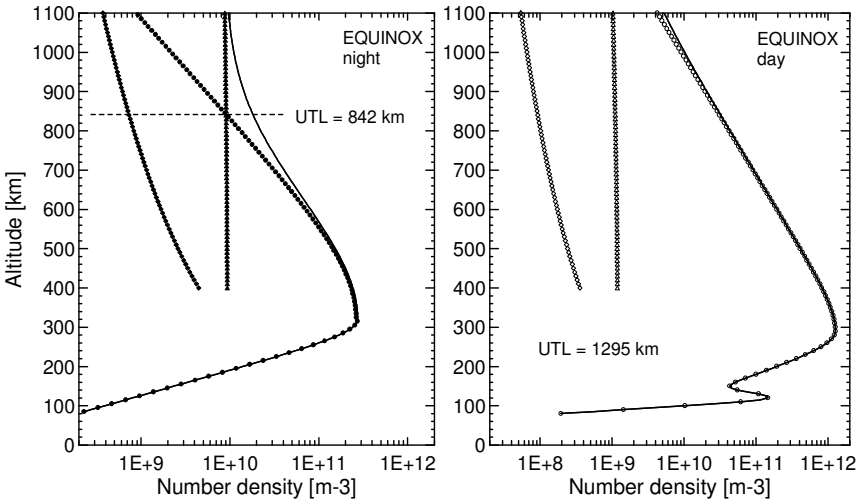

Fig.7 Vertical profiles (40°N, September equinox, F10.7=140) of the ion (symbols) and total (solid line) densities for night-time (left) and day-time (right) conditions.

All neutral atmosphere parameters required for the theoretical profiler calculations were taken from the MSIS-90 atmospheric model and presented in **Fig.6** for mid-night (left-hand panel) and mid-day (right-hand panel) conditions. Larger differences are observed for the neutral oxygen concentration and the neutral temperature during night, which leads to larger differences in the modelled density profiles. The individual and total ion densities are computed along each field line. After that, the densities were extracted at the intersecting points of these field lines and the vertical at 40°N latitude. Thus, the vertical profile at the vertical was obtained for both day and night (**Fig.7**). Integrating the calculated total ion densities along the vertical gives the ionospheric electron content – $10.5\times10^{16}[m^{-2}]$ for the night-time and $31.1\times10^{16}[m^{-2}]$ for the day-time profile.

The top-side theoretical profile provides variable scale heights for the ion density distribution which makes it much better than the simple ionospheric layers used in other IEC models. Also, the upper integration boundary is open, so the model is easily extendable to cover the total electron content. It should be reliable also because of the use of additional reference point as the upper transition height.

The constructed model is also applicable for regional mapping of the electron content. Once the density profiles are calculated along all the field lines in the latitude region, it is relatively easy to grid these profiles and to obtain the vertical density distribution (and therefore the IEC) at all points within a certain latitude interval. Applied in the same way at different longitudes, the procedure provides the IEC values over a longitude-latitude area of certain size.

8. Conclusions

Presented was a new Ionospheric Electron Content model, based on a steady-state theoretical 'ionospheric profiler' and empirical upper transition level measurements. The mathematical code is composed of coupled continuity and momentum equations of the O^+, H^+, and He^+ ions and analytical expressions for the neutral, ion and electron temperature. The IEC model can be applied for low and middle latitudes. Major advantages of this model are:

- *reliability*: top-side density distribution based on 'first-principle' model, possibilities for referencing empirical measurements (UTL, foF2).
- *flexibility*: choice of top-side profiler options for the light ions, various types of input parameters (empirical models, ionosonde measurements, satellite data), upgradeable to perform TEC calculations.
- *usability*: single-point calculations, regional mapping, model evaluations.

The accumulated ionosphere/plasmasphere monitoring data by using signals of the NNSS and GPS systems provides the possibility to evaluate the presented model which will be done in a next publication.

Acknowledgments

I thank Prof.R.Leitinger for the useful discussions and the Austrian Ministy of Science for supporting my research at the Institut für Meteorologie und Geophysik, Karl-Franzens Universität, Graz, Austria.

References

Banks, P.M., G.Kockarts, 1973. *Aeronomy*, Academic Press, New York and London.

Brown, L.D., R.E.Daniell, M.W.Fox, J.A.Klobuchar, P.H.Doherty, 1991. Evaluation of six ionospheric models as predictors of total electron content. *Radio Science* , **26**, No.4, 1007-1015.

Di Giovanni, G., S.M.Radicella, 1990. An analytical model of the electron density profile in the ionosphere, *Advances in Space Research*, Vol. **10**, No. 11, (11)27-(11)30.

Dieminger, W., G.K.Hartmann, R.Leitinger, (Eds.), 1995. *The upper atmosphere – data analysis and interpretation*, Springer, Berlin.

Dudeney, J.R., 1978. An improved model of the variation of electron concentration with height in the ionosphere, *J. Atmos. Terr. Physics*, Vol. **40**, No.2, 195-203.

Dudeney, J.R., 1983. The accuracy of simple methods for determining the height of the maximum electron concentration of the F2-layer from scaled ionospheric characteristics, *J. Atmos. Terr. Physics*, Vol. **45**, No.8/9, 629-640.

Feichter, E., R.Leitinger, 1993. *Longterm studies of ionospheric electron content*. Wissenschaftlicher Bericht No.1/1993, Institut fur Meteorologie und Geophysik, Karl-Franzens Universitat, Graz.

Kutiev, I., S.M.Stankov, 1994. Relative abundance of H^+ and He^+ in the outer ionosphere. *Advances in Space Research*, Vol. **14**, No.12, (12)139-(12)141.

Kutiev, I., S.M.Stankov, 1996. Review of progress in gathering, distributing and using satellite data for activities within COST 238 (PRIME). *Annali di Geofisica* , **39**, No.4, 775-781.

Kutiev, I., S.M.Stankov, P.Marinov, 1994. Analytical expression of O^+- H^+ transition surface for use in IRI. *Advances in Space Research*, Vol. **14**, No.12, (12)135-(12)138.

Rawer, K., 1988. Synthesis of ionospheric electron density profiles with Epstein functions. *Advances in Space Research*, Vol. **8**, No. 4, (4)191-(4)198.

Stankov, S.M., 1990. A new coordinate change in mathematical modelling of the upper ionosphere. *Comptes Rendus de l'Academie Bulgare des Sciences*, **43**, No.11, 29-31.

Stankov, S.M., 1994. *Mathematical modelling of the upper ionosphere and plasmasphere*. Ph.D. Thesis, Bulgarian Academy of Sciences, Sofia.

Stankov, S.M., 1996a. A steady-state F-region model and its use for satellite data analysis. *Annali di Geofisica* , **39**, No.5, 905-924.

Stankov, S.M., 1996b. On modelling the light-ion densities in the ionosphere. *Annali di Geofisica* , **39**, No.6, 1149-1156.

Stankov, S.M., 1996c. On the variations of daytime H^+/O^+ and He^+/O^+ ion densities during low solar activity. *Proceedings of the 1996 Conference on Solar-Terrestrial Influences*, 29 June - 3 July 1996, Sofia, Bulgaria, 29-31.

Stankov, S.M., 1999. The oxygen-helium ion transition level during low solar activity: I. Comparison of AE-C satellite data with IRI model calculations. *Bulgarian Geophysical Journal* , **25**, No.1-4, 95-116.

Stankov, S.M., 2000. The oxygen-helium ion transition level during low solar activity: II. A new empirical model. *Bulgarian Geophysical Journal* , **26**, No.1-4, 124-143.